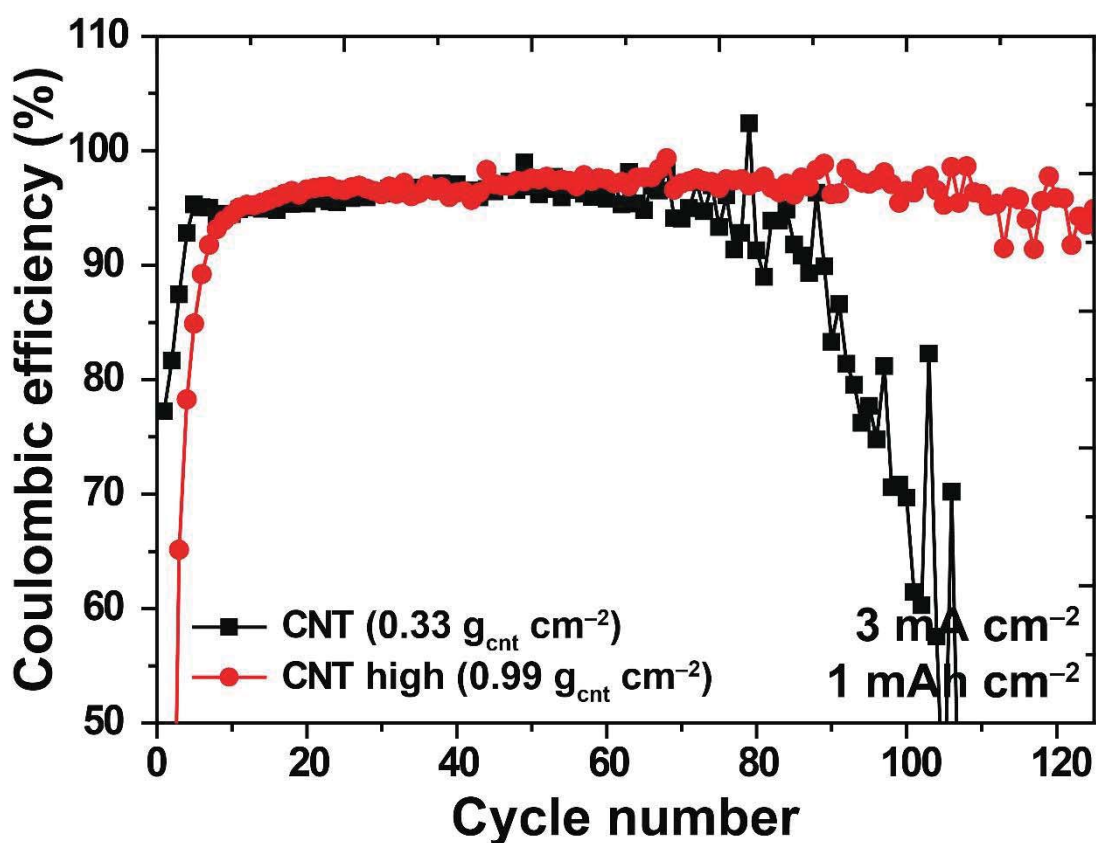


## Supporting Information

### Highly Elastic Polyrotaxane Binders for Mechanically Stable Lithium Hosts in Lithium-Metal Batteries

*Dong-Joo Yoo, Ahmed Elabd, Sunghun Choi, Yunshik Cho, Jaemin Kim, Seung Jong Lee, Seung Ho Choi, Kookheon Char, Ki Jae Kim,\* Ali Coskun,\* and Jang Wook Choi\**



**Figure S1.** Cycling performance of Li-Cu asymmetric cells with Li metal anodes containing CNT network with a mass loading of  $0.33 \text{ g}_{\text{cnt}} \text{ cm}^{-2}$  and  $0.99 \text{ g}_{\text{cnt}} \text{ cm}^{-2}$  when tested with  $1 \text{ mAh cm}^{-2}$  at  $3 \text{ mA cm}^{-2}$ . These comparative data show the importance of CNT content in sustaining its network during repeated Li uptake-release cycles.

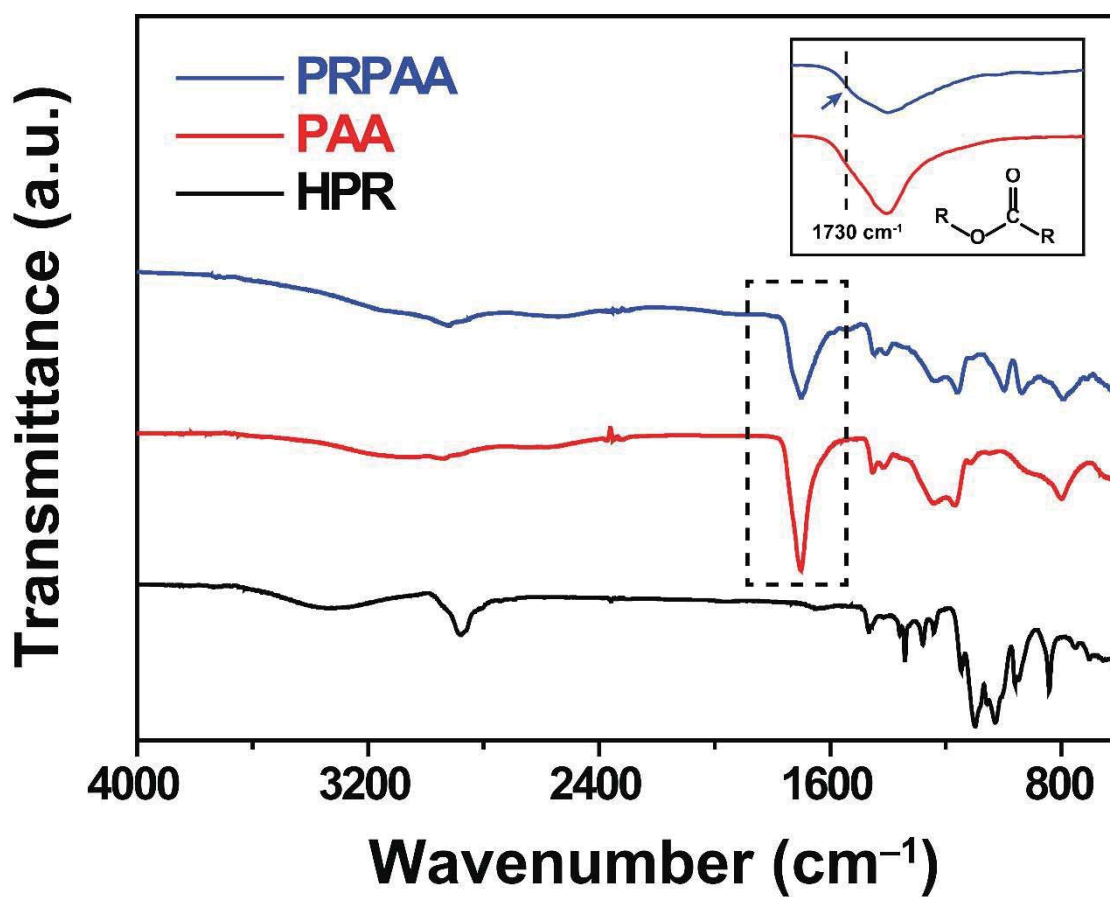


**Figure S2.** FT-IR spectra of hydroxylpropylated polyrotaxane (HPR), PAA and PRPAA. The peak of PRPAA at 1730 cm<sup>-1</sup> indicates ester linkage between PAA and HPR.

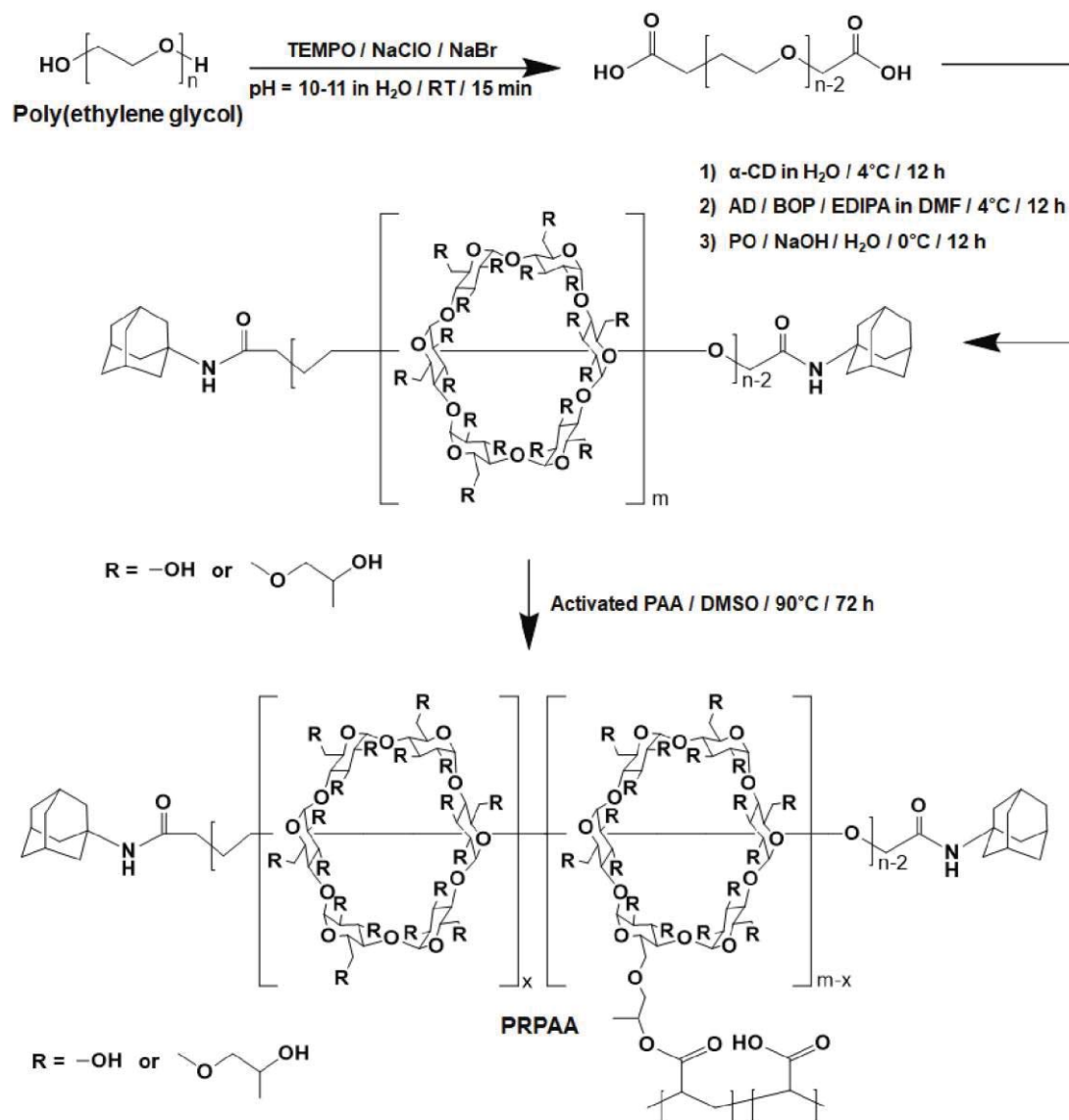
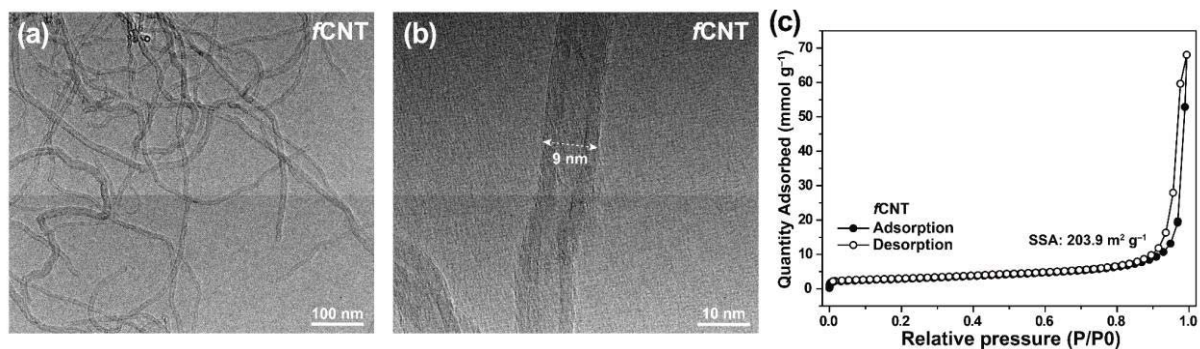
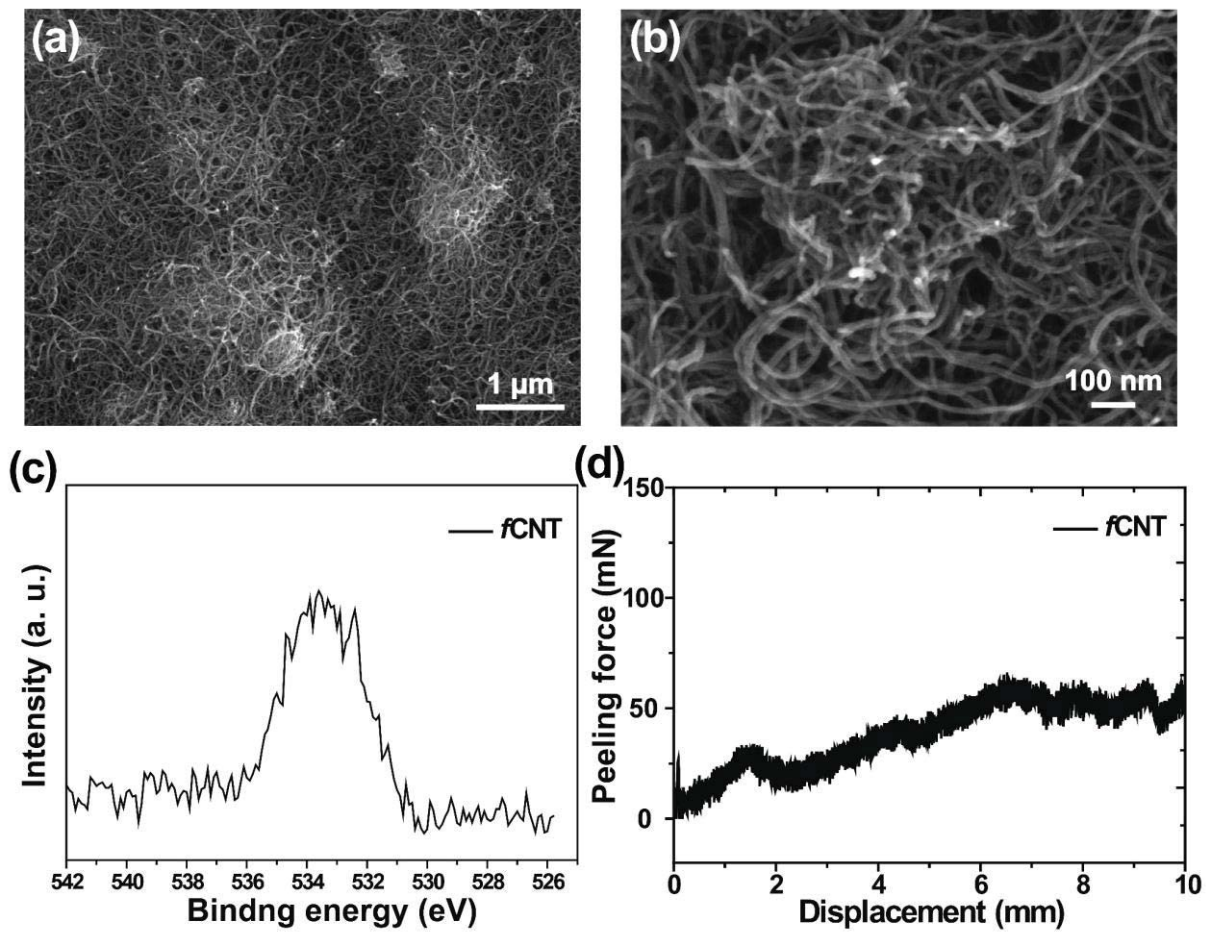


Figure S3. Synthetic scheme of PRPAA.



**Figure S4.** TEM images of *f*CNT at (a) a low magnification and (b) a high magnification. (c) BET isotherm of the same *f*CNT sample.



**Figure S5.** (a) Top-view SEM image of *f*CNT network and (b) its magnified view. (c) XPS spectrum of the *f*CNT network in O 1s branch. (d) Peeling test result of the *f*CNT network without any binder.

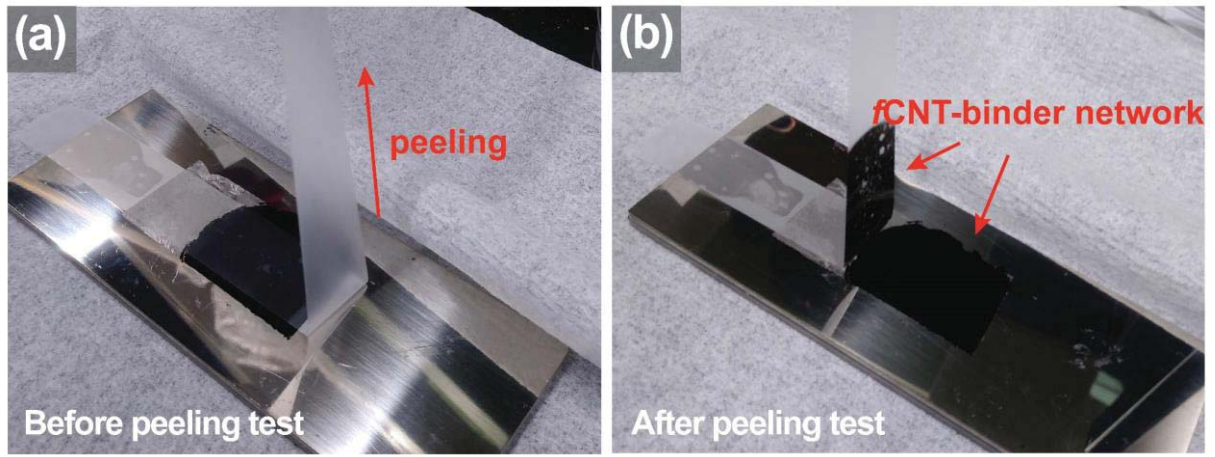


**Figure S6.** Photographs of *f*CNT-binder network (a) before and (b) after peeling test.

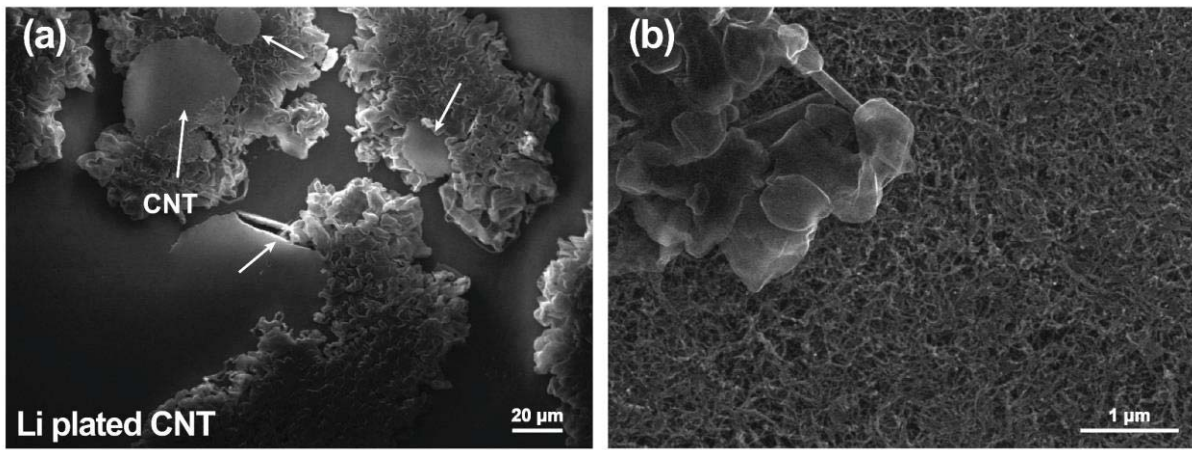


**Figure S7.** (a) SEM image of Li plated bare CNT network at  $1 \text{ mA cm}^{-2}$  (plating capacity =  $1 \text{ mAh cm}^{-2}$ ) and (b) its magnified view.

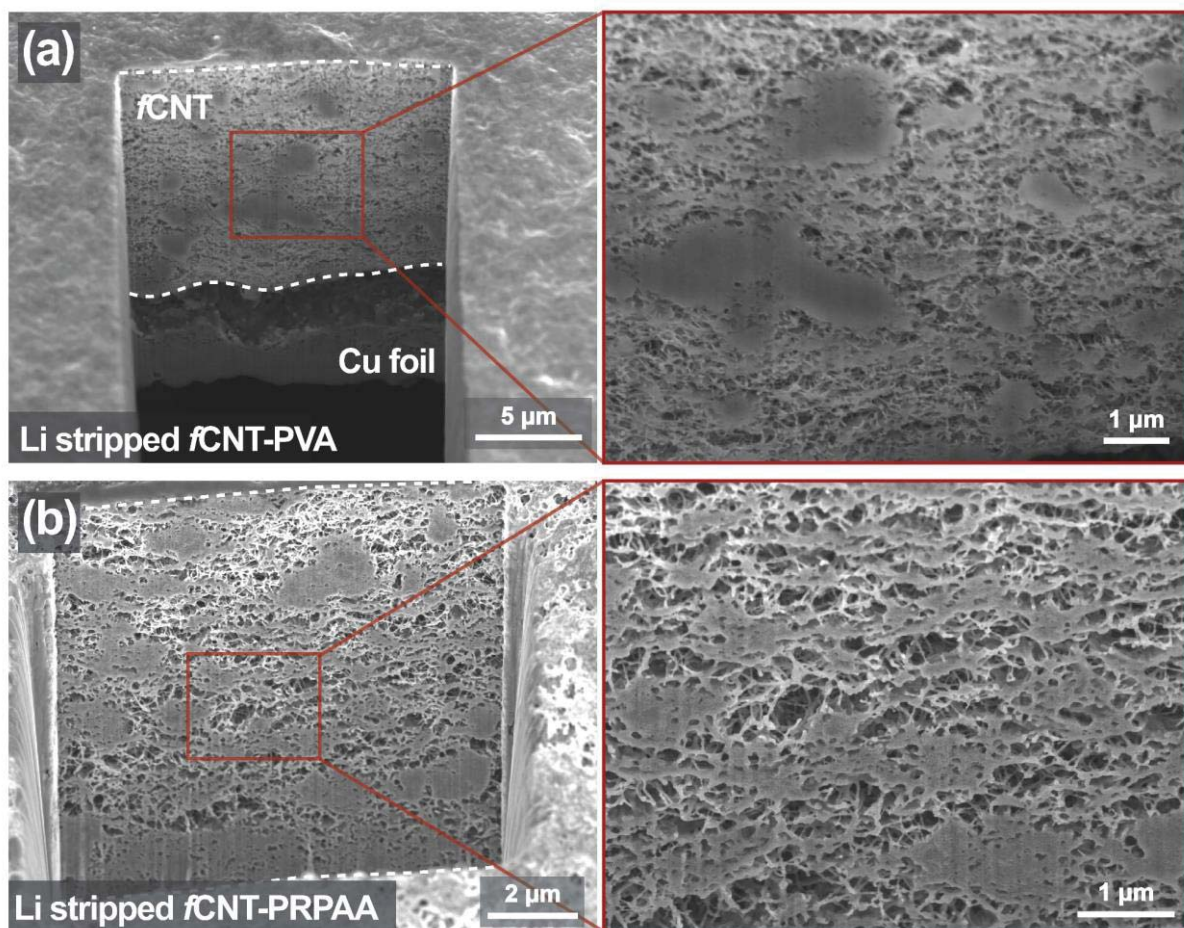


**Figure S8.** Cross-sectional SEM images of (a) *f*CNT-PVA network and (b) *f*CNT-PRPAA network after Li stripping. Current density =  $1 \text{ mA cm}^{-2}$ . Areal capacity =  $1 \text{ mAh cm}^{-2}$ .

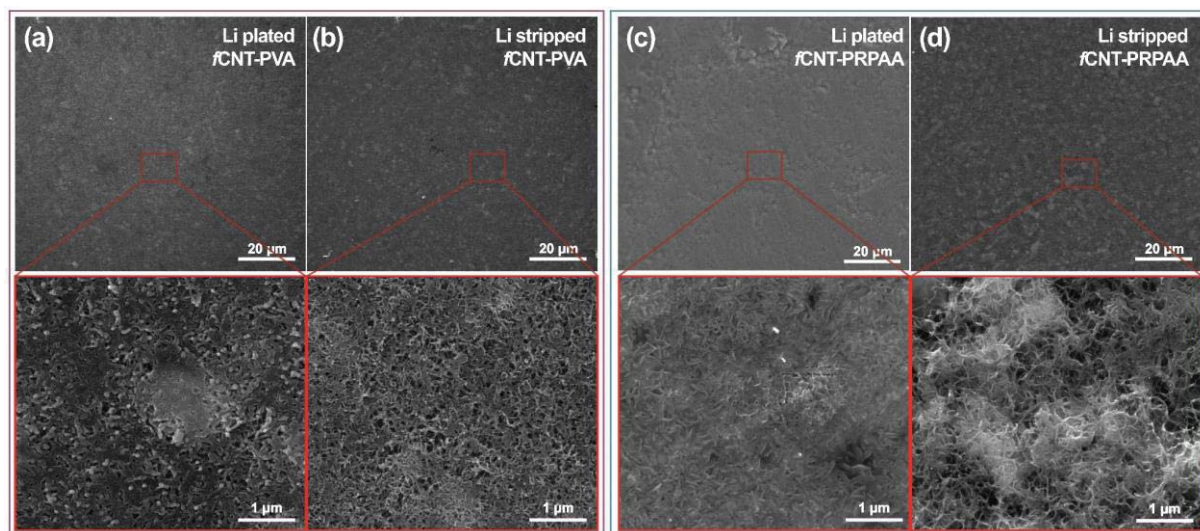


**Figure S9.** Top-view SEM images: (a) Li plated and (b) stripped *f*CNT-PVA network; (c) Li plated and (d) stripped *f*CNT-PRPAA network.

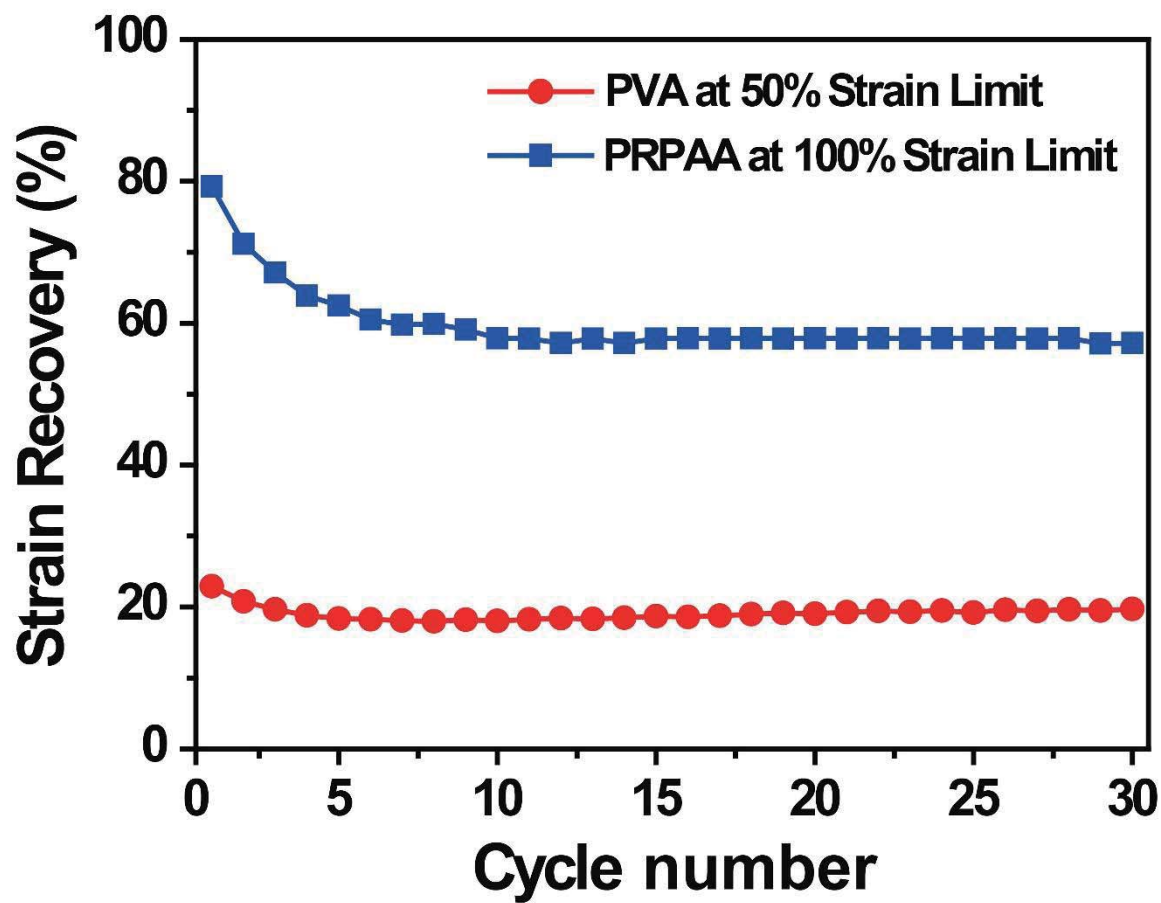


**Figure S10.** Strain recovery of PVA and PRPAA films over repeated stretch-recovery cycles. The recovery was estimated based on the formula:  $((L - L_0)/L_0) \times 100$  ( $L$ : Length of film after cycling,  $L_0$ : Length of pristine film).

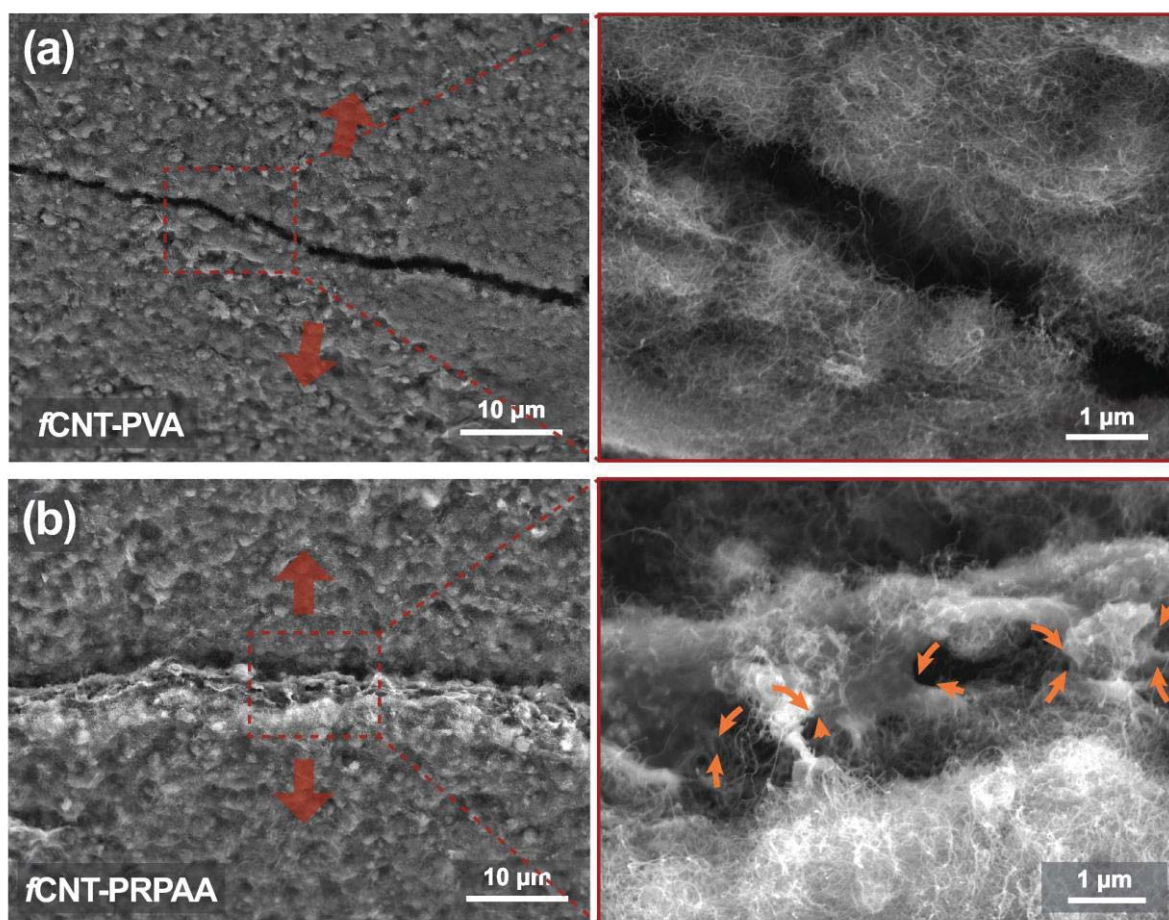


**Figure S11.** Top view SEM images of (a) *f*CNT-PVA and (b) *f*CNT-PRPAA networks when the CNT composite films were stretched until crack was generated.

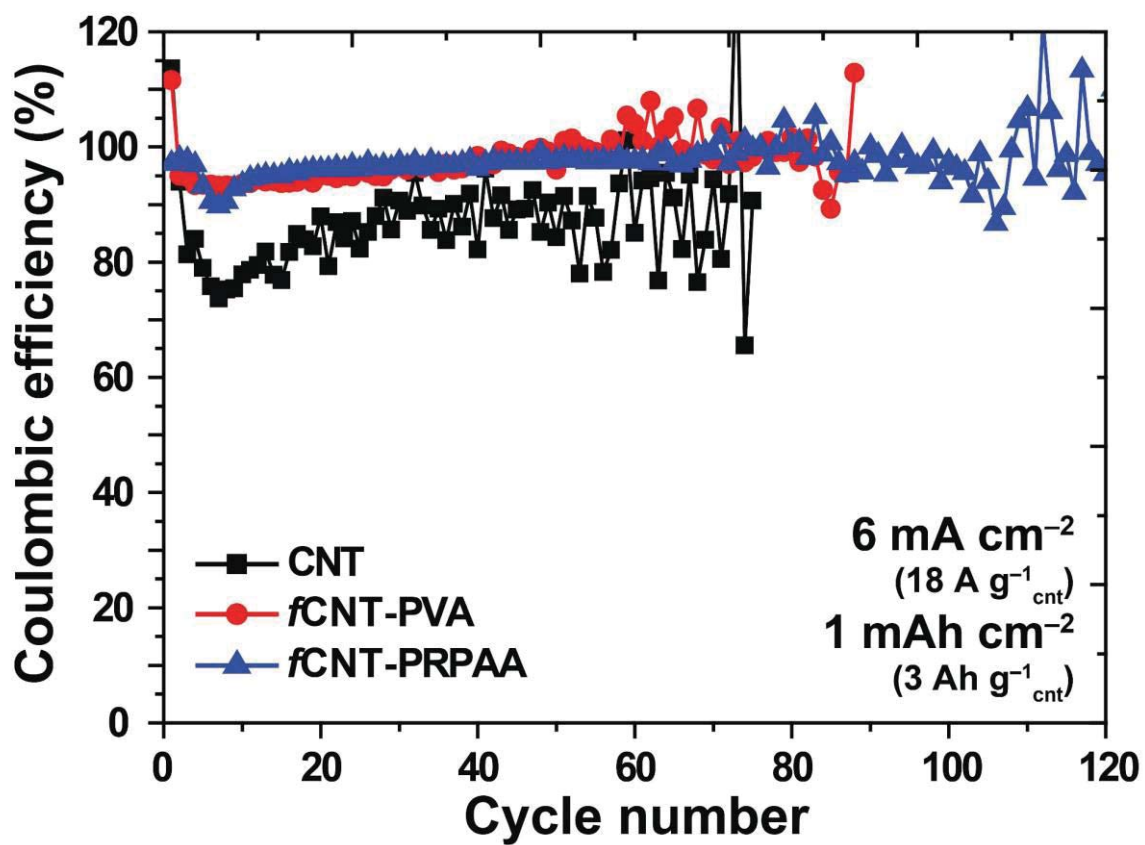


**Figure S12.** Coulombic efficiencies of Li-Cu asymmetric cells with Li metal anodes containing bare CNT, *f*CNT-PVA, and *f*CNT-PRPAA networks when tested at 6 mA cm<sup>-2</sup> with 1 mAh cm<sup>-2</sup>.

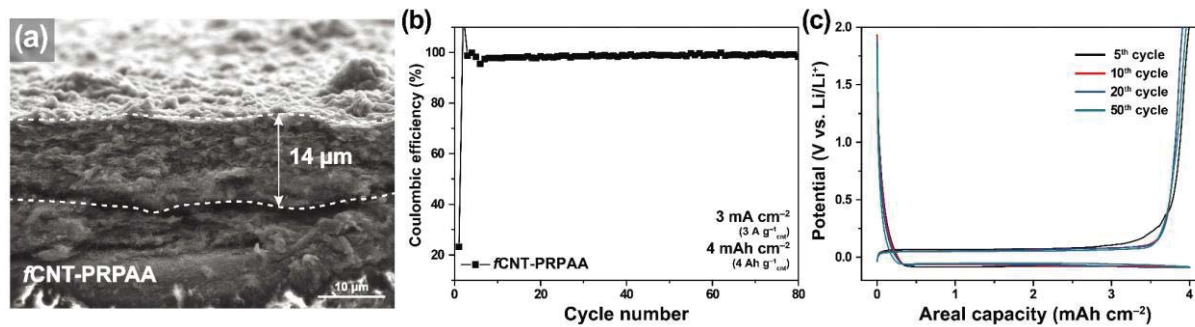


**Figure S13.** (a) Cross-sectional SEM image of a thick *f*CNT-PRPAA network. (b) Cycling performance under Li-Cu asymmetric cell mode and (c) voltage profiles of the thick *f*CNT-PRPAA electrode. Current density=3 mA cm<sup>-2</sup>. Areal capacity=4 mAh cm<sup>-2</sup>.

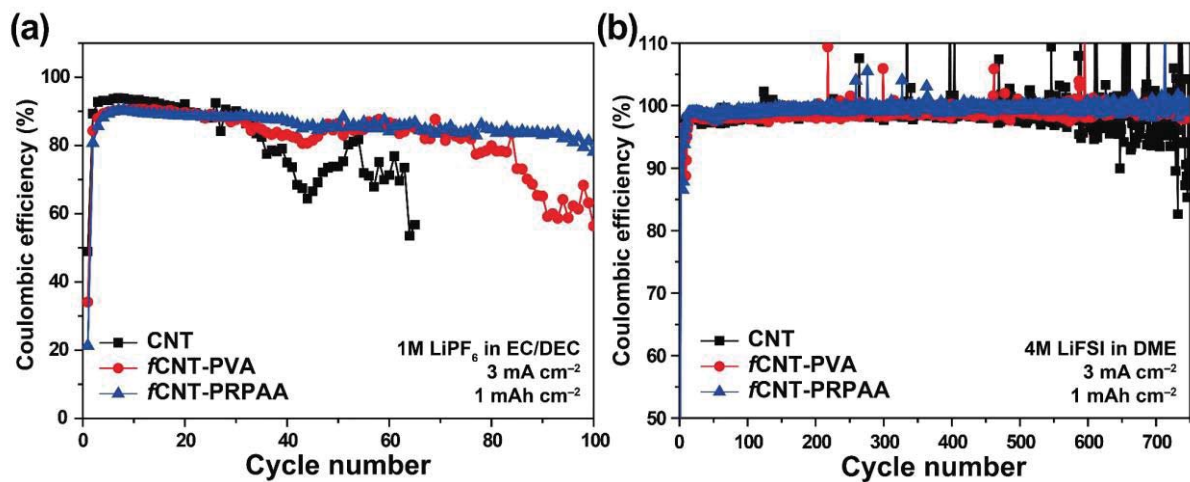


**Figure S14.** Cycling performance of Li-Cu asymmetric cells with Li metal anodes containing bare CNT network, *f*CNT-PVA network, and *f*CNT-PRPAA network with (a) 1M LiPF<sub>6</sub> in EC/DEC and (b) 4M LiFSI in DME when measured at a current density of 3 mA cm<sup>-2</sup> with a capacity of 1 mAh cm<sup>-2</sup>.

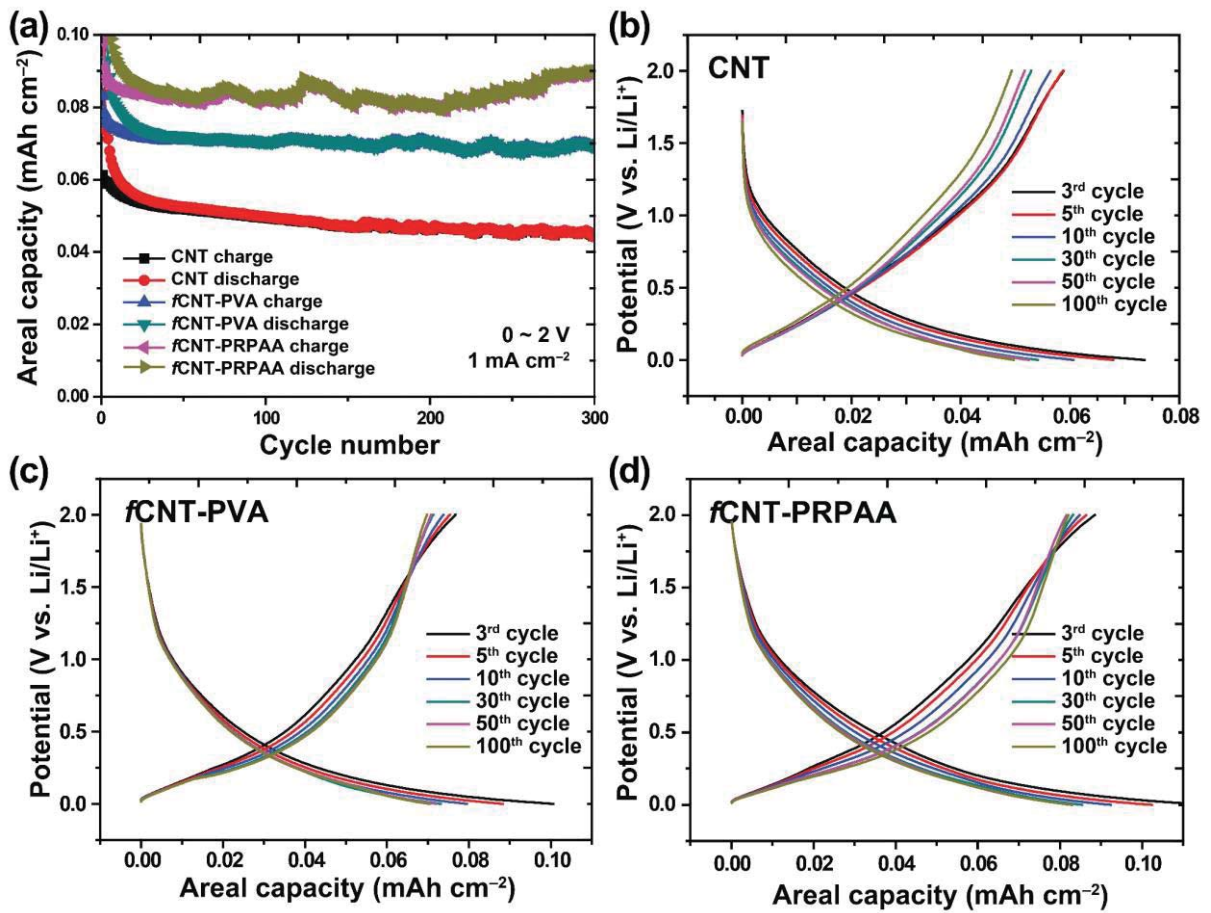


**Figure S15.** (a) Capacity retentions of bare CNT, *f*CNT-PVA, and *f*CNT-PRPAA networks when tested at  $1 \text{ mA cm}^{-2}$  in the potential range of  $0 - 2 \text{ V}$ , and (b-d) their corresponding voltage profiles at different cycles. The lower cut-off voltage of  $0 \text{ V}$  was to assess the capacitive ion storage exclusively.

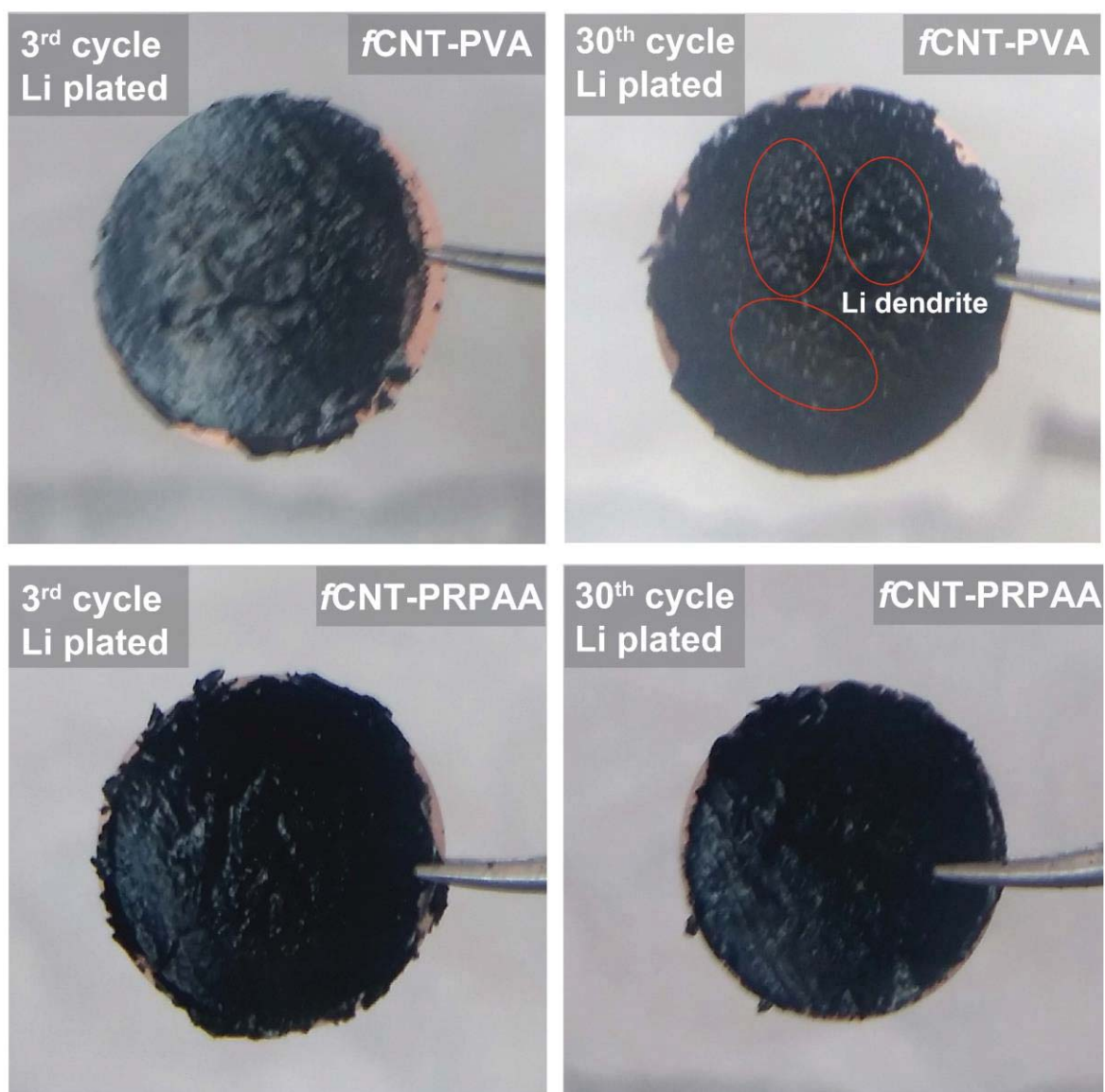


**Figure S16.** Photographs of Li plated *f*CNT-PVA and *f*CNT-PRPAA networks on the Cu foil after 3 and 30 cycles.

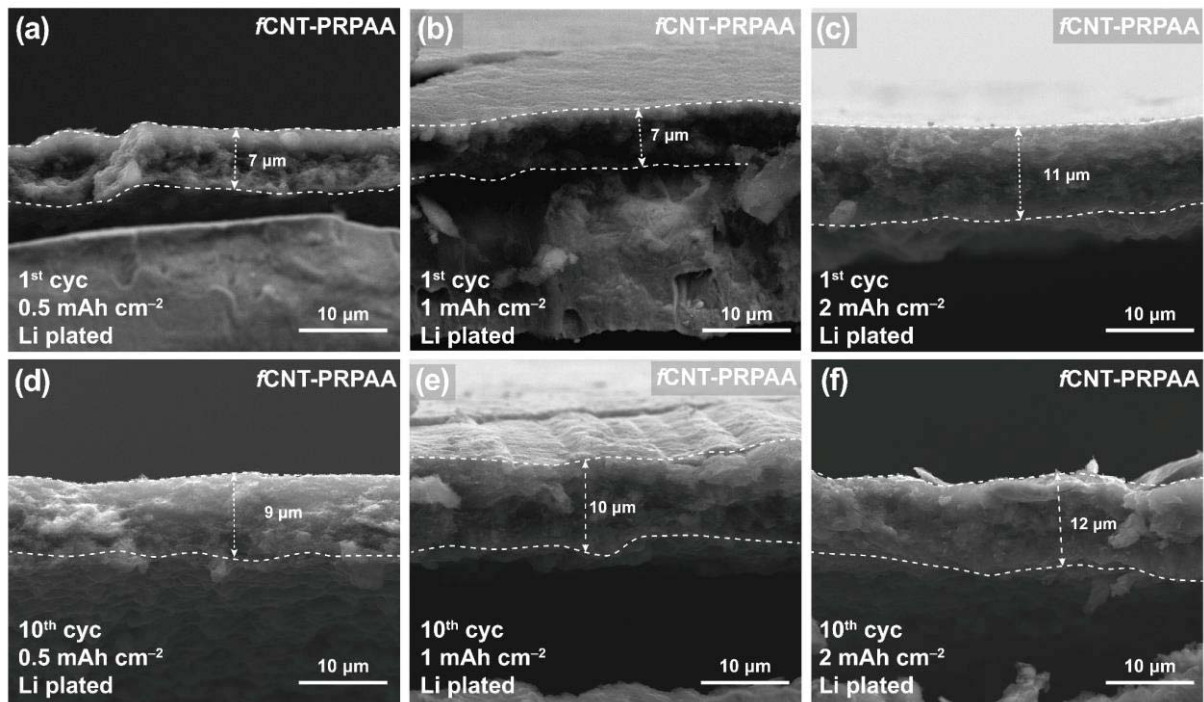


**Figure S17.** Cross-sectional SEM images of Li plated *f*CNT-PRPAA network after 1 cycle and 10 cycles with an areal capacity of (a, d)  $0.5 \text{ mAh cm}^{-2}$ , (b, e)  $1 \text{ mAh cm}^{-2}$ , and (c, f)  $2 \text{ mAh cm}^{-2}$ .

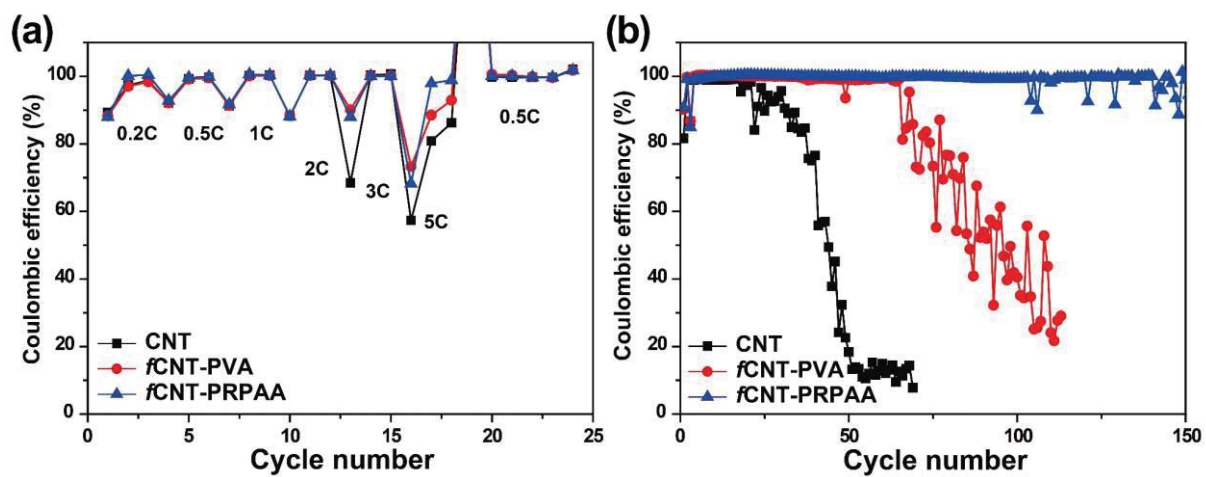


**Figure S18.** Coulombic efficiencies during (a) rate and (b) cycling performance tests for LFP-Li full cells in Figure 6.

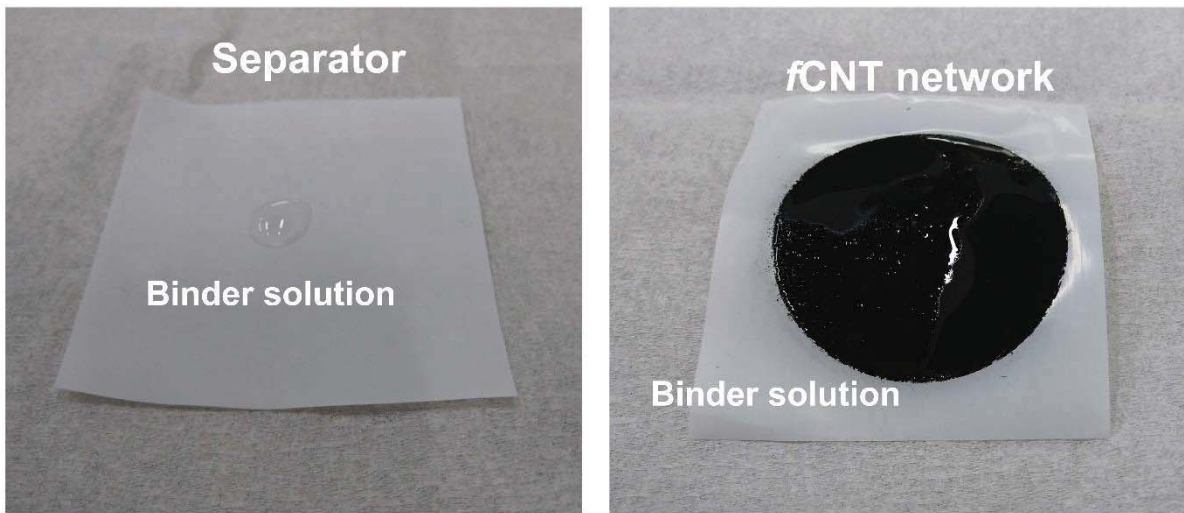


**Figure S19.** Photographs of wettability of binder solution with the separator and *f*CNT network.

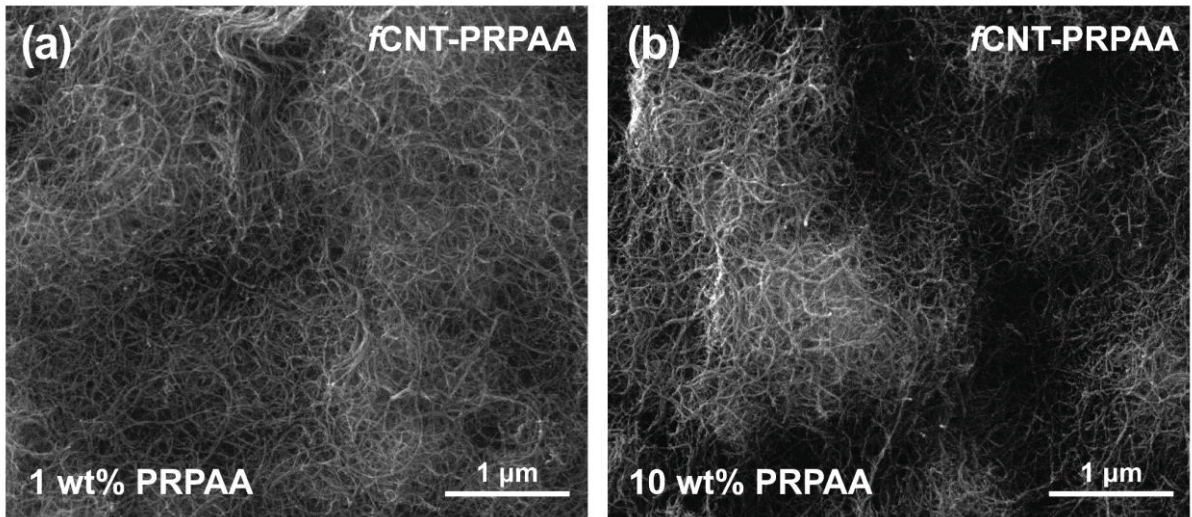


**Figure S20.** SEM images of *f*CNT-PRPAA networks with (a) 1 wt% of PRPAA and (b) 10 wt% of PRPAA.